# 3′ deletions cause aniridia by preventing *PAX6* gene expression

James D. Lauderdale*†, Jonathan S. Wilensky*, Edward R. Oliver*, David S. Walton‡, and Tom Glaser*§

*Departments of Internal Medicine and Human Genetics, University of Michigan, 4510 MSRB I, Box 0650, 1150 West Medical Center Drive, Ann Arbor, MI 48109-0650; †Department of Cellular Biology, University of Georgia, 724 Biological Sciences Building, Athens, GA 30602-2607; and ‡Massachusetts Eye and Ear Infirmary and Harvard Medical School, 2 Longfellow Place, Suite 201, Boston, MA 02114

Edited by Stanley M. Gartler, University of Washington, Seattle, WA, and approved September 29, 2000 (received for review August 18, 2000)

**Aniridia is a panocular human eye malformation caused by heterozygous null mutations within *PAX6*, a paired-box transcription factor, or cytogenetic deletions of chromosome 11p13 that encompass *PAX6*. Chromosomal rearrangements also have been described that disrupt 11p13 but spare the *PAX6* transcription unit in two families with aniridia. These presumably cause a loss of gene expression, by removing positive *cis* regulatory elements or juxtaposing negative DNA sequences. We report two submicroscopic *de novo* deletions of 11p13 that cause aniridia but are located >11 kb from the 3′ end of *PAX6*. The clinical manifestations are indistinguishable from cases with chain-terminating mutations in the coding region. Using human × mouse retinoblastoma somatic cell hybrids, we show that *PAX6* is transcribed only from the normal allele but not from the deleted chromosome 11 homolog. Our findings suggest that remote 3′ regulatory elements are required for initiation of *PAX6* expression.**

The *PAX6* transcription factor is highly conserved among metazoans and controls critical steps during eye morphogenesis (1). Human *PAX6* mutations are associated with a range of eye abnormalities, including anophthalmia, aniridia, various anterior segment defects, and isolated foveal hypoplasia (2–8). In general, heterozygosity for null alleles causes aniridia, a progressive disorder consisting of severe iris hypoplasia, cataracts, glaucoma, foveal hypoplasia, and nystagmus, whereas heterozygosity for missense alleles produces milder phenotypes (9). Aniridia is most simply explained by a 50% reduction in *PAX6* activity at the cellular level, inasmuch as most mutations are predicted to truncate the polypeptide prematurely and may trigger nonsense-mediated mRNA decay. Cases with point mutations and cytogenetic deletions (WAGR syndrome, MIM194072) have similar eye findings, and a clear dosage effect has been established among different *PAX6* genotypes (6, 10, 11). However, a dominant-negative mechanism has also been suggested for some aniridia alleles on the basis of cDNA overexpression data *in vitro* and in transgenic mice (12, 13), and an allelic inactivation model has been proposed to explain the semidominant phenotypes of most *Pax* genes (14).

Although *PAX6* is expressed abundantly in the developing eye, forebrain, ventral spinal cord, and endocrine pancreas (15–18), heterozygous phenotypes are limited to the eye. C*is* regulatory elements have been defined at the 5′ end of mouse *Pax6*. They extend over 25 kb, act upon three different promoters, include specific enhancers for retina and lens, and are evolutionarily conserved (19–21). At the same time, a paracentric inversion and a reciprocal chromosome translocation with breakpoints 85–124 kb from the 3′ end of human *PAX6* are correlated with aniridia in different pedigrees (2, 22). The relationship between the 5′ enhancer elements and 3′ *PAX6* rearrangements is unknown. In this report, we characterize two mutations as regulatory alleles, show that 3′ sequences are essential for *PAX6* expression, and establish their primacy in controlling *PAX6* transcription.

## Materials and Methods

**Cell Culture.** The human embryonic retinal cell line Ad12 (23) was kindly provided by René Bernards (Netherlands Cancer Institute, Amsterdam). The mouse retinoblastoma cell line 661 was developed from the retinal tumor of a transgenic mouse expressing SV40 large T antigen under the control of the human interphotoreceptor retinoid-binding protein (IRBP) promoter (24). 661TG$^r$ was derived from 661 by ethyl methanesulfonate mutagenesis (400 $\mu$g/ml EMS for 18 h) and selection in 5 $\mu$g/ml 6-thioguanine (25). Lymphoblastoid cell lines were established by Epstein–Barr virus transformation of peripheral white blood cells (26). Cells were fused by low-speed cocentrifugation for 3 min in serum-free media containing 40% (wt/vol) polyethylene glycol (PEG 1000; Baker). Hypoxanthine phosphoribosyl transferase-positive (HPRT$^+$) hybrid clones were selected in DMEM with 10% (vol/vol) FCS, plus hypoxanthine-aminopterin-thymidine (HAT) and 1 $\mu$M ouabain, which kill the mouse and human parental cells, respectively.

**Genomic DNA Analysis.** Pulse-field gel electrophoresis (PFGE) was performed with a hexagonal rig (CHEF Mapper; Bio-Rad). Southern analysis of conventional and pulsed-field agarose gels was performed using probes p32.1 (27), pFix2RS1 (5), pC1DBRI (an 0.5-kb *Eco*RI subclone derived from the distal breakpoint of case 1; accession no. AF301379), and P1NS (the 3′ terminal *Nco*I-*Sfi*I fragment of a 58.5-kb human P1 clone spanning *PAX6*; accession no. AF301378).

**Inverse PCR and Sequence Analysis.** Long-range inverse PCR was performed as described (28) on restricted genomic DNA that was ligated at high dilution (<100 $\mu$g/ml), using divergent primer pairs and a mixture of *Taq* and *Pwo* polymerases (EXPAND; Roche). Primers were designed on the basis of DNA sequence from phage (5) and P1 subclones. For case 1, we amplified the 3.0-kb *Eco*RI junction fragment (Fig. 1*a*). For case 2, we amplified 1.9-kb *Xba*I and 11.9-kb *Apa*I junction fragments. DNA fragments corresponding to the telomeric deletion breakpoints were obtained by screening a genomic phage library (case 1) or performing a secondary inverse PCR on normal DNA (case 2). The sequence of all four breakpoints is available from GenBank (accession nos. AF301378–81). The telomeric breakpoints of cases 1 and 2 are also represented in the public sequence database as human PAC clones (GenBank accession nos. AL135932 and AL122014, respectively).

**Haplotype Analysis.** PCR genotyping of family 2 was performed using primers flanking a polymorphic $(CA)_n$ repeat in the 3′ untranslated region of the Wilms' tumor locus *WT1* (29), which

This paper was submitted directly (Track II) to the PNAS office.

Data deposition: The sequences reported in this paper have been deposited in the GenBank database (accession nos. AF301378–AF301381).

§To whom reprint requests should be addressed. E-mail: tglaser@umich.edu.

The publication costs of this article were defrayed in part by page charge payment. This article must therefore be hereby marked "*advertisement*" in accordance with 18 U.S.C. §1734 solely to indicate this fact.

Article published online before print: *Proc. Natl. Acad. Sci. USA*, 10.1073/pnas.240398797. Article and publication date are at www.pnas.org/cgi/doi/10.1073/pnas.240398797

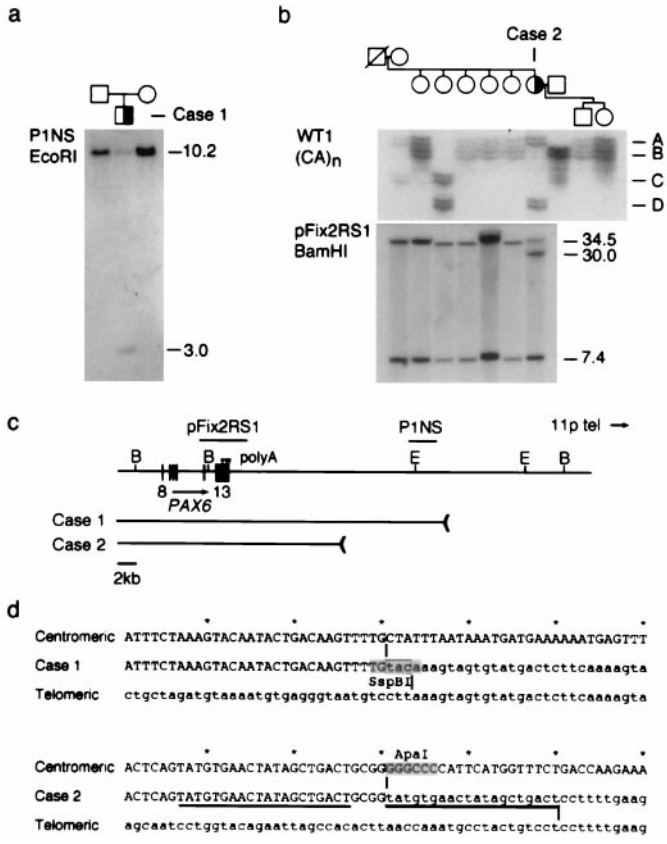


**Fig. 1.** Identification of 3′ *PAX6* rearrangements in sporadic aniridia. (*a*) Southern analysis of case 1. Probe P1NS detects a novel 3.0-kb *Eco*RI fragment in the affected child, but not in his parents, and a 10.2-kb *Eco*RI fragment in normal DNA. (*b*) Haplotype and Southern analysis of case 2. (*Upper*) Segregation of the *WT1* $(CA)_n$ repeat polymorphism. Four alleles are distinguished. Each allele is represented by an ensemble of fragments that differ from the mean length by 1–2 repeat units; these arise by replication slippage during PCR amplification. Case 2 is heterozygous (AD) at *WT1*. (*Lower*) Probe pFix2RS1 detects 34.5-kb and 7.4-kb *Bam*HI fragments in normal DNA, and an additional 30-kb *Bam*HI fragment was in the affected female, who is heterozygous. The mutation arose on a paternal chromosome 11 and is linked to *WT1* allele D. (*c*) Restriction map showing *PAX6* exons 8–13, polyadenylation sites (arrowheads), hybridization probes, and the centromeric deletion breakpoints in these two cases. The breakpoints are located 22.1 kb and 11.6 kb from the 3′ end of *PAX6*. E, *Eco*RI; B, *Bam*HI. Some of the *Eco*RI sites have been omitted. (*d*) DNA sequence spanning the centromeric (uppercase) and telomeric (lowercase) breakpoints of cases 1 and 2 in normal DNA and the deletion junctions. The junction points are indicated by vertical lines and the 20-bp duplication in case 2 is underlined. The rearrangement in case 1 creates an *Ssp*BI restriction site at the junction.

is 700 kb centromeric to *PAX6*. The wild-type chromosome 11 was identified by PCR, using primers spanning the HV translocation breakpoint at *D11S495* (30), HVnormfor (5′-CACACGGTGAAGCTAACCTATAGG-3′), and HVnormrev (5′-CAAGCTGTAGTATGCATCTC-3′), standard reaction conditions [10 mM Tris·HCl (pH 8.3), 1.5 mM $MgCl_2$, 50 mM KCl, 0.2 mM dNTPs, 20 pmol of each primer, and 1 unit *Taq* polymerase in a 50-$\mu$l volume], and parameters (2 min at 94°C, followed by 40 cycles of 30 s of denaturation at 94°C, 30 s of annealing at 60°C, and 60 s of extension at 72°C, followed by 5 min at 72°C). The mutant chromosome 11 in case 2 was identified similarly, using primers immediately flanking the deletion breakpoints, BPprox1for 5′-GTCTGCCATTCTCAACAAGGGG-3′ and BPforrev 5′-GAGGAACTGAGAAGTATTGCC-3′, and an annealing temperature of 65°C.

**RNA Analysis.** To detect *PAX6* transcripts, total RNA (2.5 $\mu$g) from somatic cell hybrids and control cell lines was reverse transcribed in 50 $\mu$l for 1 h at 42°C (SuperscriptII; GIBCO/BRL), using standard conditions and a primer (5′-TTTTTTTTTTTTT*TTA*CTGTAATCTT-3′) complementary to the human *PAX6* sequence around the stop codon. First-strand synthesis was terminated by incubating the samples at 70°C for 15 min, and the RNA was removed by treating the reactions with 2 units of RNaseH for 20 min at 37°C. PCR amplification was performed for 40 cycles in 0.2-ml thin-walled tubes, using an MJ thermocycler (MJ Research, Watertown, MA), under the conditions described above, with 1–2 $\mu$l cDNA/50-$\mu$l reaction. Cycles consisted of 30 s of denaturation at 94°C, 30 s of annealing, and 60 s of extension at 72°C, with an initial denaturation step of 2 min and a final extension step of 5 min. Human transcripts were specifically amplified using primers SCHup2 (5′-CTACCAACCAATTCCACAA-3′) from exon 10 and SCHdown1 (5′-CTTGAACTGGAACTGACACA-3′) from exon 13, and an annealing temperature of 62°C. Mouse and human transcripts were coamplified using primers 103ax (5′-TCCTTCACRTCAGGCTCCATGTTGGGC-3′) from exon 11 and 11hu (5′-CCGGGAACTTGAACTGGAAC-3′) from exon 13, and an annealing temperature of 56°C. The same first-strand cDNA products were used for both PCRs. *PAX6* polyadenylation sites were mapped using a 3′RACE procedure (31) and total RNA from human fetal eyes (17–20 weeks). PCR products were cloned, sequenced, and compared with genomic DNA. We recovered 2, 7, and 11 RACE clones corresponding to polyA sites 573 bp, 800 bp, and 967 bp, respectively, past the start of exon13.

## Results

DNA rearrangements telomeric to *PAX6* were discovered in two unrelated patients by Southern analysis (Fig. 1). Both cases are sporadic and have typical clinical features of aniridia. They are otherwise healthy and have apparently normal karyotypes. We detected a novel 3-kb *Eco*RI fragment in case 1, by using probe P1NS, which is located 19.4 kb beyond the 3′ end of *PAX6*, and a novel 30-kb *Bam*HI fragment in case 2, using probe pFix2RS1, which spans terminal exon 13. These rearrangements were also apparent when we used other restriction enzymes (not shown), but no further *PAX6* alteration was found in either patient by Southern or single-strand conformation (SSCP) analysis (5). The novel fragments were not present in parents or siblings. *WT1* haplotype analysis showed that the mutation in case 2 arose on the paternal chromosome 11 (Fig. 1*b*). To characterize the rearrangements precisely in relation to *PAX6*, the novel fragments were amplified using inverse PCRs (28) and compared with normal genomic DNA (Fig. 1*d*). *PAX6* uses three major polyadenylation sites in fetal eye tissue located 573 bp, 800 bp, and 967 bp past the start of exon 13 (not shown). The breakpoints in cases 1 and 2 were mapped 22.1 kb and 11.6 kb past the third polyA site, which defines the 3′ end of the *PAX6* transcription unit (Fig. 1*c*). Both rearrangements are interstitial deletions, inasmuch as DNA probes immediately beyond these breakpoints gave normal hybridization patterns in Southern blots, and because the novel sequences recovered by inverse PCR map to chromosome 11p (not shown). The deletion endpoints do not share extensive homology. A short tandem duplication (20 bp) of DNA from the centromeric side was observed at the junction in case 2, suggesting that replication slippage or break-induced replication accompanied this deletion (Fig. 1*d*).

To measure the size of the deletions, genomic DNA was digested with *Not*I or *Sac*II, separated by pulsed-field gel electrophoresis, and analyzed by Southern blotting (Fig. 2). In normal DNA, a 1,400-kb *Not*I fragment extends from *PAX6* toward the telomere and terminates beyond *D11S16* (2, 22, 32). This fragment was reduced to 425 kb and 295 kb, respectively, in

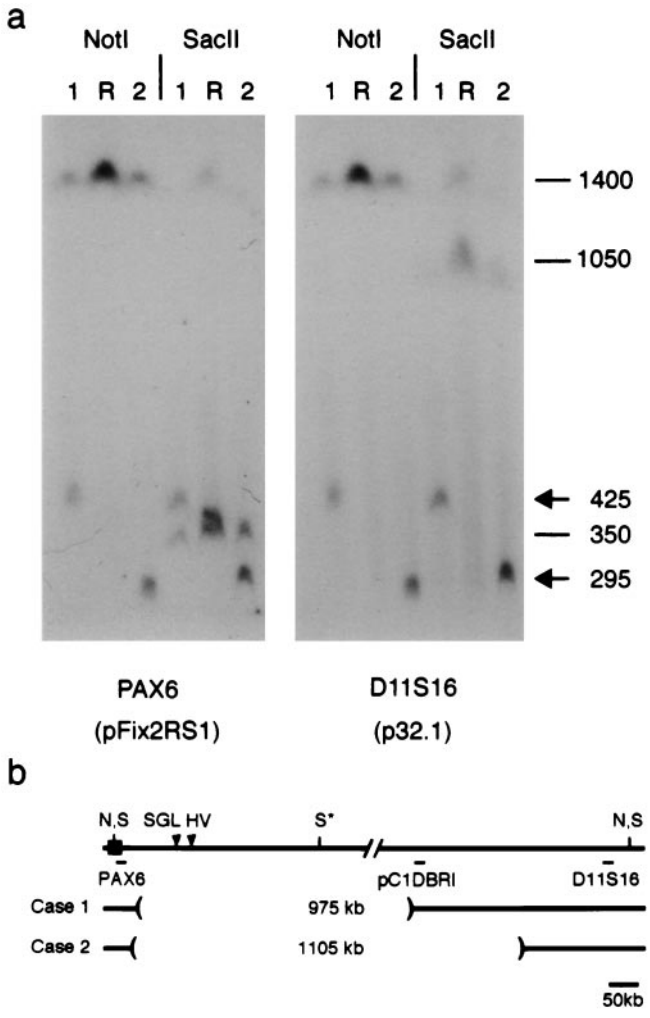


**Fig. 2.** Physical mapping of 3′ *PAX6* deletions. (*a*) Pulsed-field gel of lymphoblastoid genomic DNA from cases 1 and 2 and a normal reference individual (R) hybridized with probes pFix2RS1 and p32.1. These probes detect one 1400-kb *Not*I (N) fragment and two *Sac*II (S) fragments, which are 350 kb (centromeric) and 1050 kb (telomeric). The internal *Sac*II (S*) site is partially cleaved (22, 32). The second *Sac*II fragment in the reference (R) lane reflects a likely sequence polymorphism. (*b*) Restriction map showing hybridization probes and deletion breakpoints relative to *PAX6*. Probe pC1PBRI detects an altered *Not*I fragment in case 1 but not case 2 (data not shown). The deletions encompass breakpoints of the HV reciprocal translocation and the SGL paracentric inversion (arrowheads), which are located, respectively, 124 kb and 85–100 kb from the 3′ end of *PAX6* (22, 33, 34).

cases 1 and 2. Identical *Not*I hybridization patterns were observed with pFix2RS1 (*PAX6*) from the centromeric side and p32.1 (*D11S16*) from the telomeric side, as expected for probes flanking an internal deletion. However, the 295-kb *Not*I fragment did not hybridize with a probe (pC1DBRI) derived from the distal breakpoint of case 1 (data not shown). The deletion in case 2 thus encompasses this site. The *Sac*II data provide further support for this configuration. The internal *Sac*II restriction site is deleted in both patients, creating fragments that are similar in size to the novel *Not*I fragments and that hybridize with probes p32.1 and pFix2RS1. The deletions are 975 kb (case 1) and 1105 kb (case 2) and are nested (Fig. 2*b*). They span the breakpoints of the two large-scale chromosomal rearrangements known to cause aniridia in other pedigrees (22, 33, 34).

The simplest explanation for these combined mapping data would be if *PAX6* expression requires a positive regulatory element located >124 kb from its 3′ end, past the most distal translocation breakpoint (HV in Fig. 2*b*). To test this model and determine if the 3′ deletions affect *PAX6* transcription, we used a somatic cell hybrid strategy (35) to segregate mutant and

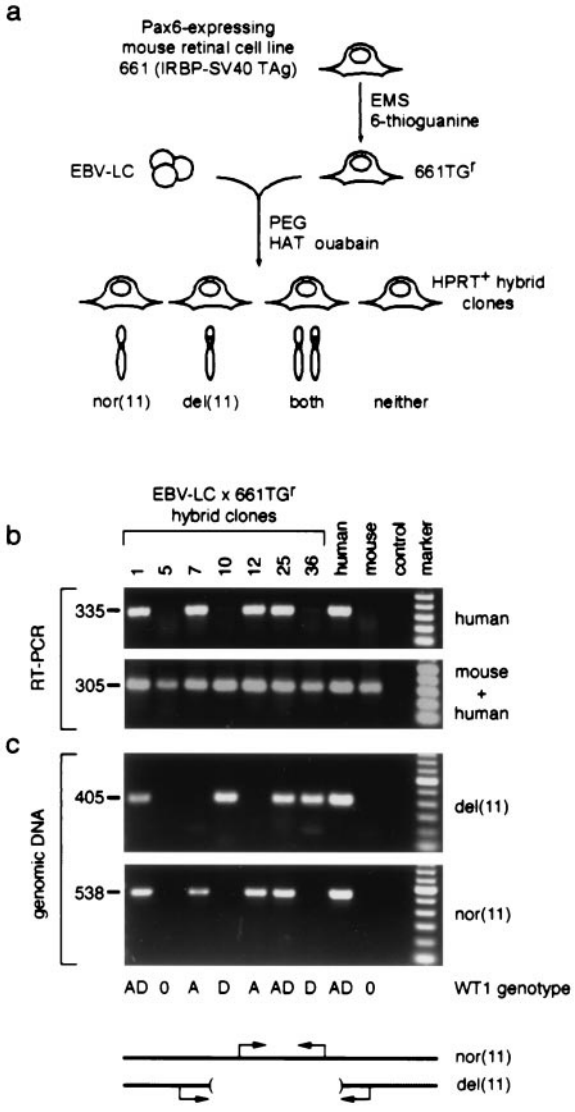


**Fig. 3.** Human *PAX6* is not expressed from the deleted chromosome 11 in somatic cell hybrids. (*a*) Strategy used to make hybrid cell lines. EBV-lymphoblastoid cells from aniridia case 2 (EBV-LC) were fused to 661TG$^r$, an HPRT-deficient mouse retinoblastoma cell line. Hybrid clones ($n$ = 37) were selected in HAT + ouabain and classified on the basis of human chromosome 11 content. In the absence of selective pressure for human autosomes, both homologs were free to segregate. (*b*) RNA analysis of representative hybrids. Human *PAX6* and mouse *Pax6* expression is demonstrated by parallel RT-PCRs, using conditions that amplify human transcripts only or transcripts from both species (see *Materials and Methods*). Hybrid clones 1, 7, 12, and 25 retain the nor(11) and express *PAX6*, whereas clones 10 and 36 retain only the del(11) and do not express *PAX6*. Similar results were obtained for all 37 clones. Reactions performed on RNA from Ad12 (human) and 661TG$^r$ (mouse) retinal cells, and a no-RT control, are shown for comparison. The size of each PCR product is indicated in base pairs. (*c*) DNA analysis of representative hybrids. The chromosome 11 content is demonstrated by diagnostic genomic PCRs. An amplicon within the deletion identifies nor(11), and an amplicon spanning the breakpoint junction identifies del(11). PCRs performed on genomic DNA from case 2 (human) and 661TG$^r$ (mouse) cells, and a no-template control reaction, are shown for comparison. *WT1* genotype data for the hybrid cell lines are indicated below the panels; the D allele is linked to the deletion. marker, 100-bp ladder (Roche); nor(11), normal; del(11), deleted.

wild-type chromosome 11 homologs. Hybrid clones were selected by fusing EBV-transformed lymphoblastoid cells from case 2 to 661TG$^r$, an HPRT-deficient mouse retinoblastoma cell line with a high level of endogenous *Pax6* expression (Fig. 3*a*). Clones retaining mutant and wild-type chromosomes 11 were identified by allele-specific PCR (Fig. 3*c*) and *WT1* genotype analysis (Fig. 1*b*). Among 37 hybrid clones, 4 retained only the wild-type chromosome 11 and 8 retained only the deleted chromosome 11, whereas 21 clones retained both homologs and 4 retained neither. We then tested *PAX6* expression, using a human-specific reverse transcriptase (RT) PCR assay. Although expression of mouse *Pax6* was maintained in all clones, only hybrids retaining a normal chromosome 11 ($n = 25$) expressed human *PAX6* (Fig. 3*b* and data not shown). The cellular environment of the mouse somatic cell hybrids is thus sufficient to activate and maintain transcription of the human *PAX6* gene. However, *PAX6* was essentially silent in all eight hybrids retaining only the mutated copy of chromosome 11, even though the gene itself is intact and the RT-PCR is extremely sensitive. The correlation between the *PAX6* genotype and expression is absolute (for 12 clones retaining one homolog, for Fisher's exact test, $P < 0.002$, df = 1), and the difference in expression is striking.

## Discussion

Our data prove that 3′ deletions prevent *PAX6* expression in *cis*. The tight correlation among the somatic cell hybrids between genotype and expression is inconsistent with an allelic inactivation model, which predicts a random inactivation of *PAX6* alleles among the hybrid clones (14). Together with the clinical, structural, and 3′ RACE data, these results strongly suggest that the deletions affect *PAX6* transcription rather than mRNA stability. There is no evidence for a remote untranslated 3′ exon and no need to invoke a second independent aniridia gene within 11p13. Our results also provide further support for haploinsufficiency as the basis of aniridia rather than a dominant-negative mechanism. Finally, these findings are comparable to earlier results obtained using somatic cell hybrids for deletions of the β-globin locus control region (LCR) in $\delta\beta\gamma^o$-thalassemia (36). The on-off effect of the 3′ deletion upon *PAX6* transcription is consistent with clinical findings in these two patients, whose disease differs from that of patients with documented partial loss-of-function alleles (9) and suggests the workings of an LCR or an array of critical enhancers, which could influence the transcriptional activity of adjoining chromatin regions in an all-or-none fashion (37, 38). This hypothesis is supported by the convergence of mapping data on the 3′ side of *PAX6*, including experiments in which a human YAC transgene spanning *PAX6* was able to rescue the *Small eye* mouse phenotype if the 3′ flanking DNA was intact (11). Alternatively, the deletions may disrupt a specific insulator or boundary element that normally shields the *PAX6* transcription unit (39). The discontinuous nature of our results is less consistent with gene silencing via nonspecific position effects (40, 41) or the fractional loss of tissue-specific enhancer elements, which has been suggested to explain the milder phenotypes of translocation cases for genetic diseases such as holoprosencephaly (*SHH*) or Saethre–Chotzen syndrome (*TWIST*; refs. 42 and 43) and remote 3′ deletions altering the expression of *Bmp5* in mice and *dpp* in *Drosophila* (44, 45). All known *eyeless* mutations in *Drosophila Pax6* are regulatory alleles (46). We have functionally characterized *cis* regulatory alleles of human *PAX6*. The molecular identity and properties of the 3′ element(s) should be particularly interesting.

We thank the patients and their families for participating in the study; René Bernards, Muayyad Al-Ubaidi, and Anand Swaroop for cell lines; David Kurnit for loaning PFGE equipment; Hua Li and David Law for technical assistance; Richard Maas for help in the initial stages of this project; Gail Bruns, Manfred Gessler, and Tom Wilson for valuable advice; and David Burke, David Ginsburg, John Moran, and Diane Robins for critically reading the manuscript. This work was supported by grants from the National Institutes of Health and the Howard Hughes Medical Institute to T.G.

1. Gehring, W. J. & Ikeo, K. (1999) *Trends Genet.* **15,** 371–377.
2. Ton, C. C., Hirvonen, H., Miwa, H., Weil, M. M., Monaghan, P., Jordan, T., van Heyningen, V., Hastie, N. D., Meijers-Heijboer, H., Drechsler, M., *et al.* (1991) *Cell* **67,** 1059–1074.
3. Hanson, I., Jordan, T. & Van Heyningen, V. (1994) in *Molecular Genetics of Inherited Eye Disorders*, eds. Wright, A. F. & Jay, B. (Harwood Academic, Switzerland), pp. 445–467.
4. Prosser, J. & van Heyningen, V. (1998) *Hum. Mutat.* **11,** 93–108.
5. Glaser, T., Walton, D. S. & Maas, R. L. (1992) *Nat. Genet.* **2,** 232–239.
6. Glaser, T., Jepeal, L., Edwards, J. G., Young, S. R., Favor, J. & Maas, R. L. (1994) *Nat. Genet.* **7,** 463–471.
7. Hanson, I. M., Fletcher, J. M., Jordan, T., Brown, A., Taylor, D., Adams, R. J., Punnett, H. H. & van Heyningen, V. (1994) *Nat. Genet.* **6,** 168–173.
8. Azuma, N., Nishina, S., Yanagisawa, H., Okuyama, T. & Yamada, M. (1996) *Nat. Genet.* **13,** 141–142.
9. Hanson, I., Churchill, A., Love, J., Axton, R., Moore, T., Clarke, M., Meire, F. & van Heyningen, V. (1999) *Hum. Mol. Genet.* **8,** 165–172.
10. Hill, R. E., Favor, J., Hogan, B. L., Ton, C. C., Saunders, G. F., Hanson, I. M., Prosser, J., Jordan, T., Hastie, N. D. & van Heyningen, V. (1991) *Nature (London)* **354,** 522–525.
11. Schedl, A., Ross, A., Lee, M., Engelkamp, D., Rashbass, P., van Heyningen, V. & Hastie, N. D. (1996) *Cell* **86,** 71–82.
12. Singh, S., Tang, H. K., Lee, J. Y. & Saunders, G. F. (1998) *J. Biol. Chem.* **273,** 21531–21541.
13. Duncan, M. K., Cvekl, A., Li, X. & Piatigorsky, J. (2000) *Invest. Ophthalmol. Vis. Sci.* **41,** 464–473.
14. Nutt, S. L. & Busslinger, M. (1999) *Biol. Chem.* **380,** 601–611.
15. Walther, C. & Gruss, P. (1991) *Development (Cambridge, U.K.)* **113,** 1435–1449.
16. Grindley, J. C., Davidson, D. R. & Hill, R. E. (1995) *Development (Cambridge, U.K.)* **121,** 1433–1442.
17. Ericson, J., Morton, S., Kawakami, A., Roelink, H. & Jessell, T. M. (1996) *Cell* **87,** 661–673.
18. St-Onge, L., Sosa-Pineda, B., Chowdhury, K., Mansouri, A. & Gruss, P. (1997) *Nature (London)* **387,** 406–409.
19. Williams, S. C., Altmann, C. R., Chow, R. L., Hemmati-Brivanlou, A. & Lang, R. A. (1998) *Mech. Dev.* **73,** 225–229.
20. Kammandel, B., Chowdhury, K., Stoykova, A., Aparicio, S., Brenner, S. & Gruss, P. (1999) *Dev. Biol.* **205,** 79–97.
21. Xu, P. X., Zhang, X., Heaney, S., Yoon, A., Michelson, A. M. & Maas, R. L. (1999) *Development (Cambridge, U.K.)* **126,** 383–395.
22. Fantes, J., Redeker, B., Breen, M., Boyle, S., Brown, J., Fletcher, J., Jones, S., Bickmore, W., Fukushima, Y., Mannens, M., *et al.* (1995) *Hum. Mol. Genet* **4,** 415–422.
23. Vaessen, R. T., Houweling, A., Israel, A., Kourilsky, P. & van der Eb, A. J. (1986) *EMBO J.* **5,** 335–341.
24. Al-Ubaidi, M. R., Font, R. L., Quiambao, A. B., Keener, M. J., Liou, G. I., Overbeek, P. A. & Baehr, W. (1992) *J. Cell Biol.* **119,** 1681–1687.
25. Hsie, A. W., Brimer, P. A., Mitchell, T. J. & Gosslee, D. G. (1975) *Somatic Cell Genet.* **1,** 247–261.
26. Anderson, M. A. & Gusella, J. F. (1984) *In Vitro* **20,** 856–858.
27. Feder, J., Yen, L., Wijsman, E., Wang, L., Wilkins, L., Schroder, J., Spurr, N., Cann, H., Blumenberg, M. & Cavalli-Sforza, L. L. (1985) *Am. J. Hum. Genet.* **37,** 635–649.
28. Ochman, H., Medhora, M. M., Garza, D. & Hartl, D. L. (1990) in *PCR Protocols: A Guide to Methods and Applications*, eds. Innis, M., Gelfand, D., Sninsky, J. & White, T. (Academic, San Diego), pp. 219–227.
29. Haber, D. A., Buckler, A. J., Glaser, T., Call, K. M., Pelletier, J., Sohn, R. L., Douglass, E. C. & Housman, D. E. (1990) *Cell* **61,** 1257–1269.
30. Gessler, M., Simola, K. O. & Bruns, G. A. (1989) *Science* **244,** 1575–1578.
31. Frohman, M. A. (1990) in *PCR Protocols: A Guide to Methods and Applications* (Academic, San Diego), pp. 28–38.
32. Gessler, M. & Bruns, G. A. (1989) *Genomics* **5,** 43–55.
33. Simola, K. O., Knuutila, S., Kaitila, I., Pirkola, A. & Pohja, P. (1983) *Hum. Genet.* **63,** 158–161.
34. Fukushima, Y., Hoovers, J., Mannens, M., Wakui, K., Ohashi, H., Ohno, T., Ueoka, Y. & Niikawa, N. (1993) *Hum. Genet.* **91,** 205–209.
35. Weiss, M. C. & Green, H. (1967) *Proc. Natl. Acad. Sci. USA* **58,** 1104–1111.
36. Forrester, W. C., Epner, E., Driscoll, M. C., Enver, T., Brice, M., Papayannopoulou, T. & Groudine, M. (1990) *Genes Dev.* **4,** 1637–1649.

37. Bulger, M. & Groudine, M. (1999) *Genes Dev.* **13,** 2465–2477.
38. Engel, J. D. & Tanimoto, K. (2000) *Cell* **100,** 499–502.
39. Bell, A. C. & Felsenfeld, G. (1999) *Curr. Opin. Genet. Dev.* **9,** 191–198.
40. Bedell, M. A., Jenkins, N. A. & Copeland, N. G. (1996) *Nat. Genet.* **12,** 229–232.
41. Kleinjan, D. J. & van Heyningen, V. (1998) *Hum. Mol. Genet.* **7,** 1611–1618.
42. Belloni, E., Muenke, M., Roessler, E., Traverso, G., Siegel-Bartelt, J., Frumkin, A., Mitchell, H. F., Donis-Keller, H., Helms, C., Hing, A. V., *et al.* (1996) *Nat. Genet.* **14,** 353–356.
43. Krebs, I., Weis, I., Hudler, M., Rommens, J. M., Roth, H., Scherer, S. W., Tsui, L. C., Fuchtbauer, E. M., Grzeschik, K. H., Tsuji, K., *et al.* (1997) *Hum. Mol. Genet.* **6,** 1079–1086.
44. DiLeone, R. J., Russell, L. B. & Kingsley, D. M. (1998) *Genetics* **148,** 401–408.
45. Masucci, J. D., Miltenberger, R. J. & Hoffmann, F. M. (1990) *Genes Dev.* **4,** 2011–2023.
46. Quiring, R., Walldorf, U., Kloter, U. & Gehring, W. J. (1994) *Science* **265,** 785–789.